UMTA-MA-06-0025-81-6
DOT-TSC-UMTA-81-75

Harmonic Characteristics of Rectifier Substations and Their Impact on Audio Frequency Track Circuits
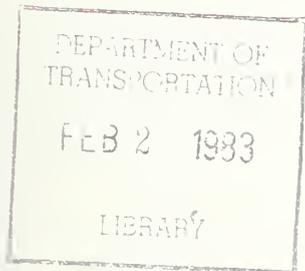
Vilas D. Nene

OAO Corporation
7500 Greenway Center
Greenbelt MD 20770

May 1982
Final Report

This document is available to the public
through the National Technical Information
Service, Springfield, Virginia 22161.

U.S. Department of Transportation

Urban Mass Transportation Administration

Office of Technical Assistance
Office of Systems Engineering
Washington DC 20590

1. Report No. UMTA-MA-06-0025-81-6	2. Government Accession No.	3. Recipient's Catalog No.

4. Title and Subtitle Harmonic Characteristics of Rectifier Substations and Their Impact on Audio Frequency Track Circuits		5. Report Date May 1982
		6. Performing Organization Code DTS-722
7. Author's) Vilas D. Nene, Ph.D.		8. Performing Organization Report No. DOT-TSC-UMTA-81-75
9. Performing Organization Name and Address OAO Corporation* 7500 Greenway Center Greenbelt, Maryland 20770		10. Work Unit No. (TRAIS) UM204/R2616
		11. Contract or Grant No. DTRS-57-81-C-00033
12. Sponsoring Agency Name and Address U.S. Department of Transportation Urban Mass Transportation Administration Office of Technical Assistance Washington DC 20590		13. Type of Report and Period Covered Final Report 1/15/1981 - 7/15/1981
		14. Sponsoring Agency Code URT-10

15. Supplementary Notes
*Under contract to: U.S. Department of Transportation
Research and Special Programs Administration
Transportation Systems Center
Cambridge MA 02142

16. Abstract

This report describes the basic operation of substation rectifier equipment and the modes of possible interference with audio frequency track circuits used for train detection, cab signalling and vehicle speed control. It also includes methods of estimating EM noise received by track circuits from substation operation.

17. Key Words Rectifiers, Substation Harmonics, Electromagnetic Interference	18. Distribution Statement DOCUMENT IS AVAILABLE TO THE U.S. PUBLIC THROUGH THE NATIONAL TECHNICAL INFORMATION SERVICE, SPRINGFIELD, VIRGINIA 22161

19. Security Classif. (of this report) UNCLASSIFIED	20. Security Classif. (of this page) UNCLASSIFIED	21. No. of Pages 54	22. Price

Form DOT F 1700.7 (8-72)   Reproduction of completed page authorized

PREFACE

METRIC CONVERSION FACTORS

Approximate Conversions to Metric Measures

Symbol	When You Know	Multiply by	To Find	Symbol
		LENGTH		
in	inches	*2.5	centimeters	cm
ft	feet	30	centimeters	cm
yd	yards	0.9	meters	m
mi	miles	1.6	kilometers	km
		AREA		
in^2	square inches	6.5	square centimeters	cm^2
ft^2	square feet	0.09	square meters	m^2
yd^2	square yards	0.8	square meters	m^2
mi^2	square miles	2.6	square kilometers	km^2
	acres	0.4	hectares	ha
		MASS (weight)		
oz	ounces	28	grams	g
lb	pounds	0.45	kilograms	kg
	short tons (2000 lb)	0.9	tonnes	t
		VOLUME		
tsp	teaspoons	5	milliliters	ml
Tbsp	tablespoons	15	milliliters	ml
fl oz	fluid ounces	30	milliliters	ml
c	cups	0.24	liters	l
pt	pints	0.47	liters	l
qt	quarts	0.96	liters	l
gal	gallons	3.8	liters	l
ft^3	cubic feet	0.03	cubic meters	m^3
yd^3	cubic yards	0.76	cubic meters	m^3
		TEMPERATURE (exact)		
°F	Fahrenheit temperature	5/9 (after subtracting 32)	Celsius temperature	°C

*1 in = 2.54 (exactly). For other exact conversions and more detailed tables, see NBS Misc. Publ. 286. Units of Weights and Measures. Price $2.25. SD Catalog No. C13.10.286.

Approximate Conversions from Metric Measures

Symbol	When You Know	Multiply by	To Find	Symbol
		LENGTH		
mm	millimeters	0.04	inches	in
cm	centimeters	0.4	inches	in
m	meters	3.3	feet	ft
m	meters	1.1	yards	yd
km	kilometers	0.6	miles	mi
		AREA		
cm^2	square centimeters	0.16	square inches	in^2
m^2	square meters	1.2	square yards	yd^2
km^2	square kilometers	0.4	square miles	mi^2
ha	hectares (10,000 m^2)	2.5	acres	
		MASS (weight)		
g	grams	0.035	ounces	oz
kg	kilograms	2.2	pounds	lb
t	tonnes (1000 kg)	1.1	short tons	
		VOLUME		
ml	milliliters	0.03	fluid ounces	fl oz
l	liters	2.1	pints	pt
l	liters	1.06	quarts	qt
l	liters	0.26	gallons	gal
m^3	cubic meters	35	cubic feet	ft^3
m^3	cubic meters	1.3	cubic yards	yd^3
		TEMPERATURE (exact)		
°C	Celsius temperature	9/5 (then add 32)	Fahrenheit temperature	°F

°F   −40   0   32   80   98.6   120   160   200   212 °F
°C   −40   −20   0   20   37   40   60   80   100 °C

iv

TABLE OF CONTENTS

LIST OF FIGURES

EXECUTIVE SUMMARY

A typical transit substation has two or more diode rectifiers with a combined power rating of 2-10 MW. With a very few exceptions, these are 3-phase 12-pulse rectifier circuits. Under normal operating conditions with balanced voltage inputs, these rectifiers cause harmonic currents in the third rail with harmonic orders of multiples of 12. For example, with a source frequency of 60 Hz as in the U.S., the third rail carries current harmonics with frequencies of 720 Hz, 1440 Hz, 2160 Hz,..., etc. Because of inherent unbalance in voltage inputs as well as some asymmetry in bridge circuits, the third rail also carries current components with frequencies of 60 Hz, 120 Hz, ... etc., although of reduced magnitudes.

These substation harmonics in the third rail cause electromagnetic (EM) noise in the audio frequency track circuits, resulting in potential circuit malfunction. This report describes the basic operation of substation rectifier equipment and the modes of possible interference with the track circuits. It also presents methods of estimating electromagnetic noise levels in the track circuits caused by the substation rectifiers.

The substation harmonic frequencies are well defined and are independent of other wayside and vehicle equipment. The amplitudes of these harmonic currents in the third rail are highest when a train is near a feeding point on the third rail. The EM noise levels in the track circuit caused by rectifier harmonics are, however, minimum when the length of running rails in the propulsion circuit is minimum. This is because the propulsion return current is then likely to be shared equally by the two

running rails in a two-rail circuit, and the induction from the third rail is minimum, since the length of the exposed circuit is small. Protection against substation harmonics is not necessary when rail lengths are short and currents are small except in site-specific problem areas such as the third rail switching sides at bonds, etc., or under abnormal conditions such as loose connections, etc. These problems must then be investigated on an individual basis.

1. INTRODUCTION

Research and development programs of the Urban Mass Transportation Administration (UMTA) in the area of urban rail transit have been recently restructured. These programs collectively known as STARS, Subsystem Technology Applications to Rail Systems, include vehicle systems, wayside equipment, operational aspects, etc., and now focus on the cost effectiveness and near-term application of rail transit technology.

Study of electromagnetic interference (EMI) characteristics of propulsion and other solid state power conversion equipment is a part of the STARS program. Various track circuit configurations and electromagnetic compatibilities of chopper and inverter controlled propulsion systems have been investigated in earlier studies[1-4]. The reader is, therefore, assumed to be familiar with track circuits and electromagnetic compatibility in general.

This report describes the basic operation of substation rectifier equipment and the modes of possible interference with audio frequency track circuits used for train detection, cab signalling and vehicle speed control. It also includes methods of estimating EM noise received by track circuits from substation operation.

2. THREE PHASE BRIDGE RECTIFIERS

A three phase bridge rectifier shown in Figure 2-1 is one of the most widely used converter connections. The three phase voltage input at a,b,c may be obtained via a distribution transformer with star or delta connected windings on the primary and secondary side. The rectifier operation and the loading characteristic essentially are independent of transformer connection. The waveform of line current in the ac network is, of course, directly related to the type of transformer connection used.

Now consider a balanced three phase voltage system connected at abc in Figure 2-1. The load on the rectifier is highly inductive, causing current I_d in the load to be constant generally. If the diodes D1, D2, --D6 are ideal, they conduct the load current when they are forward biased, and they block it when they are reverse biased. With reference to the voltages of Figure 2-2, when the voltage V_{ab} is positive and larger in magnitude than V_{cb} and V_{ac}, the diodes D6 and D1 are forward biased and conduct the load current; the voltage V_d across the load is then identically equal to V_{ab}. When, however, V_{ac} is positive and higher than V_{ab} and V_{bc}, the diodes D1 and D2 conduct and the voltage V_d equals V_{ac}. Thus each pair of diodes conducts in turn for 60 electrical degrees, as shown in Figure 2-2. Each diode conducts for 120 electrical degrees in each cycle of the input voltages. In this bridge connection, current transfer from one diode to another occurs six times every input cycle. This rectifier is, therefore, called a six-pulse rectifier.

When the diode D1 conducts, $i_a = I_d$, but when D4 conducts $i_a = -I_d$; therefore, the waveform of line currents i_a, i_b, and i_c is defined by the

2
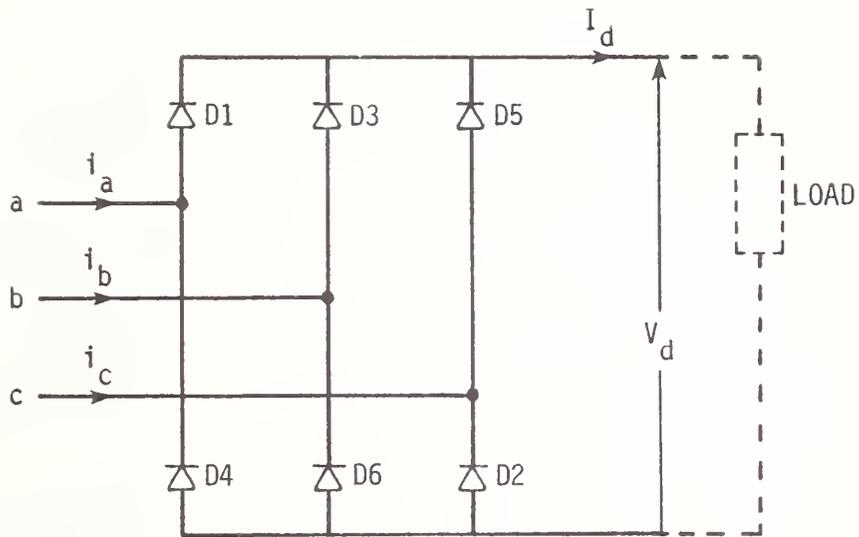
FIGURE 2-1. Three Phase Bridge Rectifier
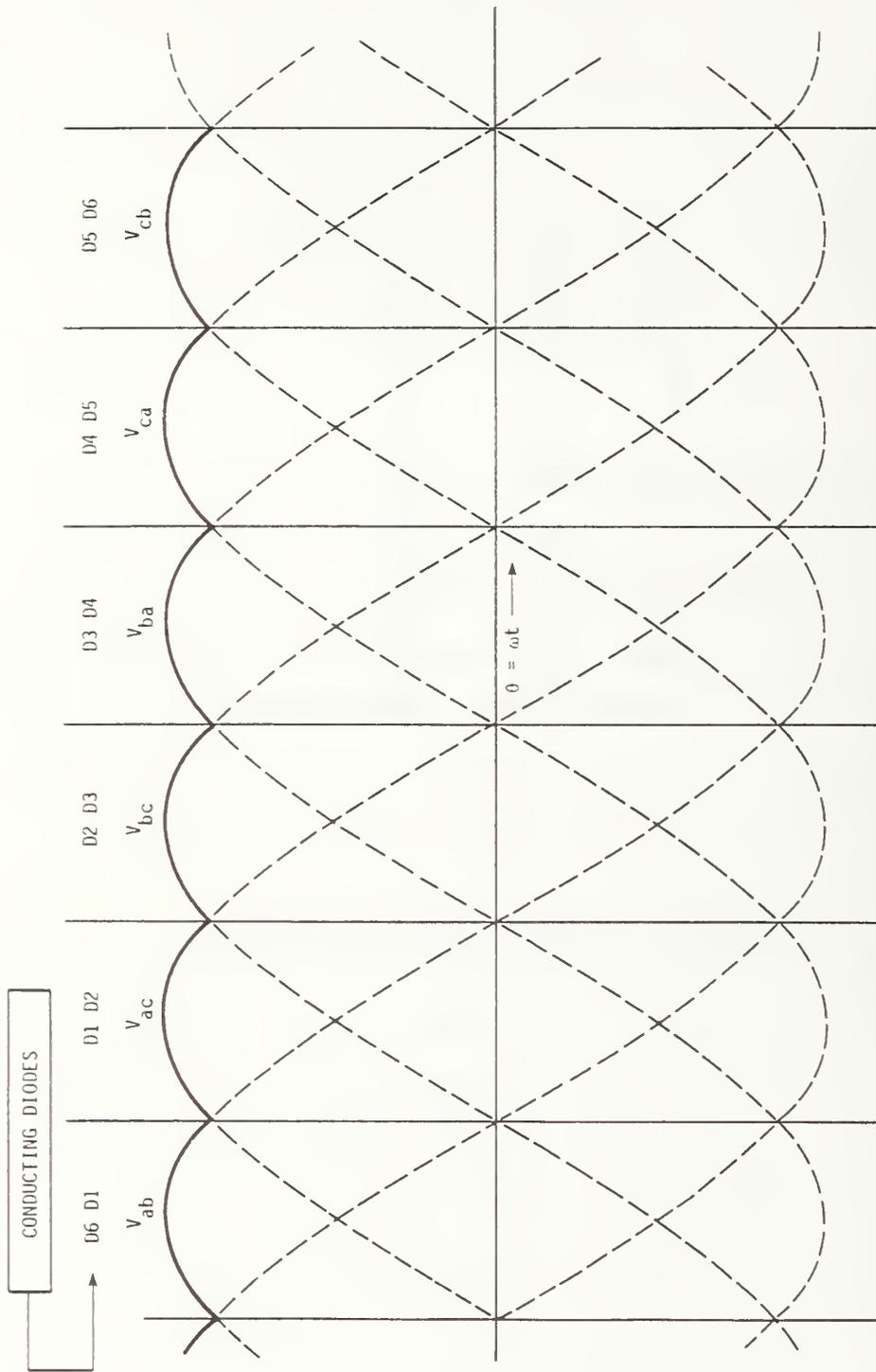
FIGURE 2-2. Balanced Three Phase Voltages

4

conduction pattern for diodes. These currents appear in Figure 2-3. The waveforms of current in the transformer windings on primary and secondary sides are obtainable from these line currents for any given winding connection. For example, on the secondary side, the winding currents are:

$$i_p = i_a \text{ for star connection}$$

$$\text{and} \quad i_p = 1/3(i_a - i_b) \text{ for delta connection.}$$

These waveforms appear in Figure 2-4.

2.1 COMMUTATION PROCESS

The transfer of load current from one diode to another is called 'commutation'. In the preceding discussion this commutation was assumed instantaneous. Some commutation reactance is, however, associated with the ac source side of the bridge circuit. The load current commutation, consequently, takes a finite period of time. The process clarifies with the help of Figure 2-5.

Assume that diodes D1 and D2 are conducting, and that the output voltage V_d is equal to V_{ac}. At the time t=o, V_{ba} becomes positive and the diode D3 is forward biased. A loop current i_{cc} then flows as shown in Figure 2-5a. If the resistance in the circuit and the voltage drop across the diodes are neglected, then:

$$2X_c \frac{di_{cc}}{d\theta} = v_{ba} = V \sin\theta$$

5
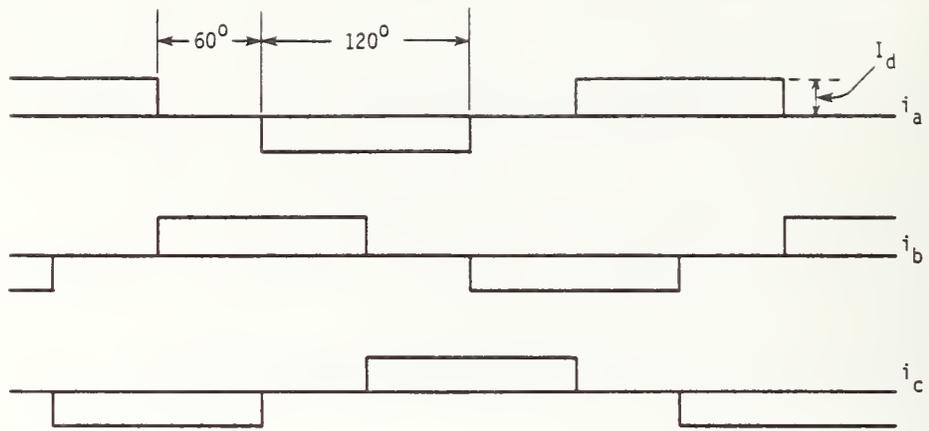
FIGURE 2-3.   Line Current Waveforms

DELTA CONNECTION

STAR CONNECTION
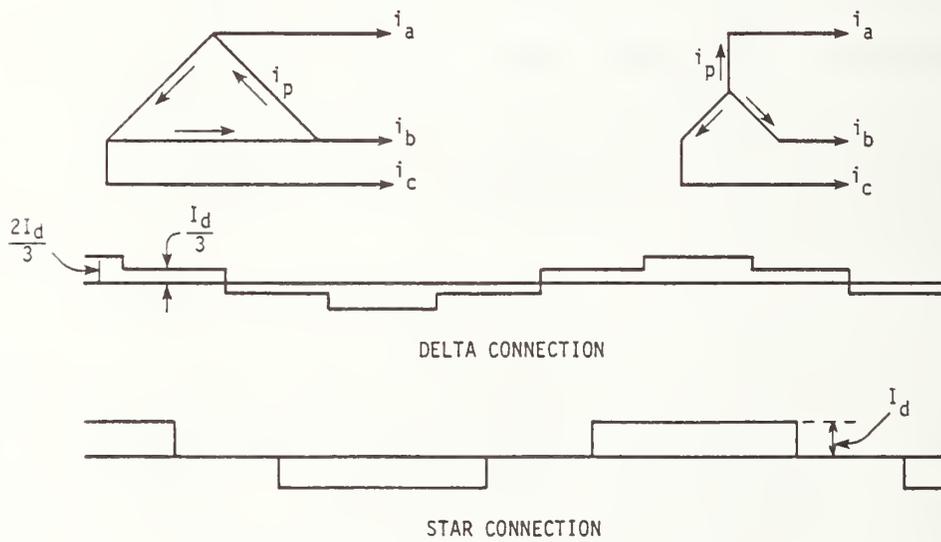
FIGURE 2-4.   Transformer Secondary Phase Currents

(a) COMMUTATION CURRENT

(b) VOLTAGE WAVEFORM
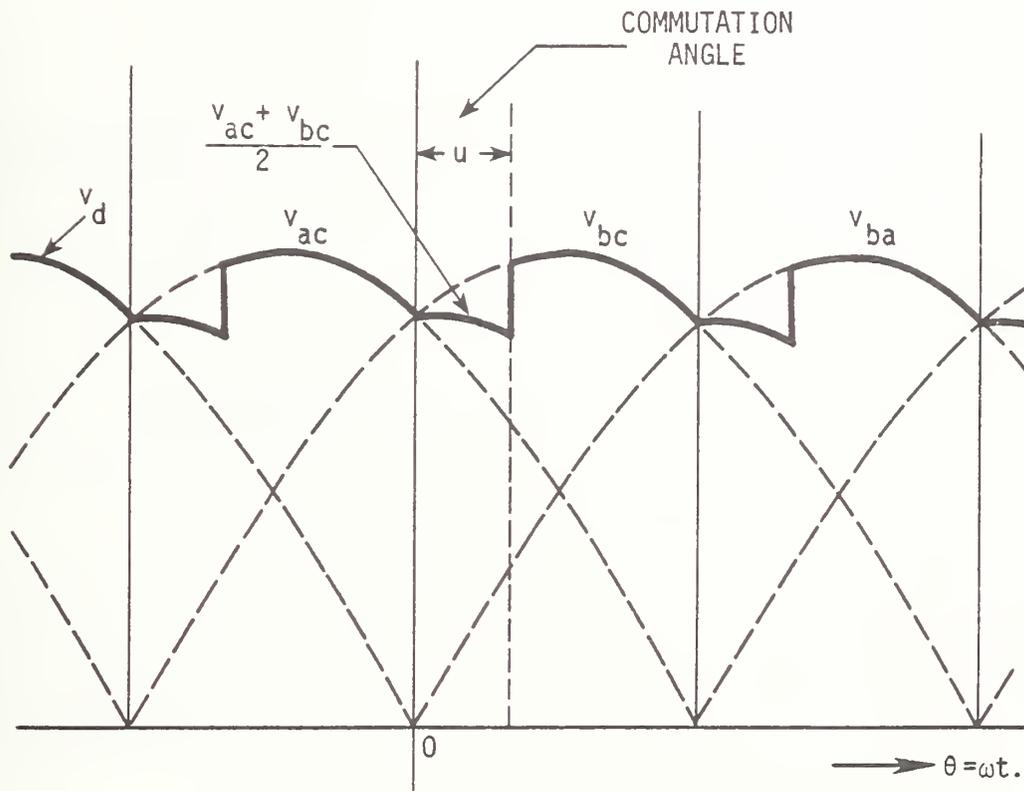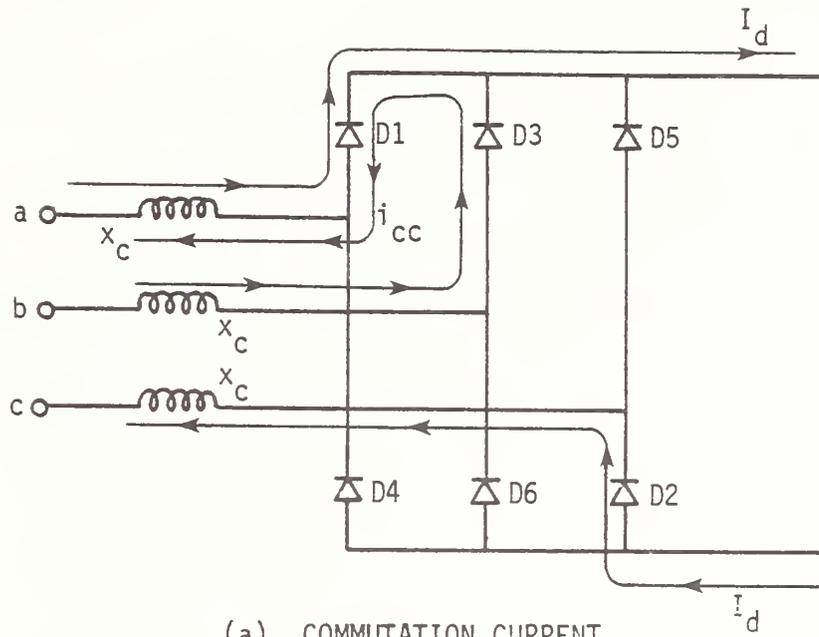
FIGURE 2-5. Commutation Process

7

with the initial condition that $i_{cc} = 0$ at $\Theta = 0$, and:

$$i_{cc} = \frac{V}{2X_c} (1 - \cos\Theta)$$

When this current i_{cc} equals I_d, the current in D1 is zero, and the transfer of current from D1 to D3 is complete. The commutation angle u, also called the overlap angle, is then given by the equation:

$$I_L = \frac{V}{2X_c} (1 - \cos u),$$

i.e.,

$$u = \cos^{-1} (1 - \frac{2X_c I_L}{V}$$

The reactance X_c is the sum of the per phase leakage reactance of the transformer, line reactance, any current dividing chokes, and stray reactance, if any.

During the commutation period, the output voltage appears as:

$$V_d = V_{ac} + i_{cc}X_c = V_{ac} + \tfrac{1}{2}V_{ba},$$

and because:

$$V_{ab} + V_{bc} + V_{ca} = 0$$

$$V_d = \tfrac{1}{2}(V_{ac} + V_{bc}).$$

8

2.2 OUTPUT VOLTAGE WAVEFORM

The output voltage of the rectifer is periodic over $\pi/3$. The voltage waveform now is formulated as:

$$v_d = \frac{\sqrt{3}}{2} \; V \; \cos\theta \qquad \text{for} \quad o \leqslant \theta \leqslant u$$

$$= V \sin\left(\theta + \frac{\pi}{3}\right) \qquad \text{for} \quad u \leqslant \theta \leqslant \frac{\pi}{3}$$

The average value of this output voltage is:

$$V_d = \frac{3V}{2\pi} \; (1 + \cos u)$$

If the commutation reactance is zero, u equals zero and maximum average output voltage is:

$$V_{do} = \frac{3V}{\pi}$$

Harmonic components of this waveform are also obtainable by standard techniques. These are:

$$V_{dm \; rms} = \frac{3V}{\pi(m^2 - 1)} \cdot \frac{1}{\sqrt{2}} \cdot MAG \; [(1 - \cos u \; e^{jmu}) - jm \sin u \; e^{jmu}]$$

where MAG(Z) is the absolute value of a complex variable Z, and m can only be a multiple of six.

It can be seen that for u = o

$$V_{dm \; rms} = \frac{3V}{\pi} \left(\frac{\sqrt{2}}{m^2 - 1}\right)$$

Fig. 2-6 presents relative rms values of harmonic components of the output voltage for different commutation angles. The harmonic orders presented here cover a broad range of frequency (0-10 kHz), to enable approximate evaluation of any possible impact of these harmonics on audio frequency track circuits used on the U.S. transit systems.

2.3 VOLTAGE REGULATION

The average dc output voltage of the rectifier reduces as the load current is increased. Basically two components comprise this voltage drop:

(a) commutation component: As the load current increases, the overlap angle u increases resulting in reduced output;

(b) ohmic loss component: With increased load current, the copper losses in transformer, reactors and other components increase and cause a drop in voltage output.

Any voltage drop across the conducting diode elements is quite independent of the load current. It does not therefore, affect the regulation characteristic of the rectifier, although the voltage output is reduced by this voltage drop as in Figure 2-7.

2.4 OPERATION WITH UNBALANCED VOLTAGE INPUT

The earlier sections assumed that the rectifier was supplied with a balanced three phase voltage source. The output voltage, therefore,

10
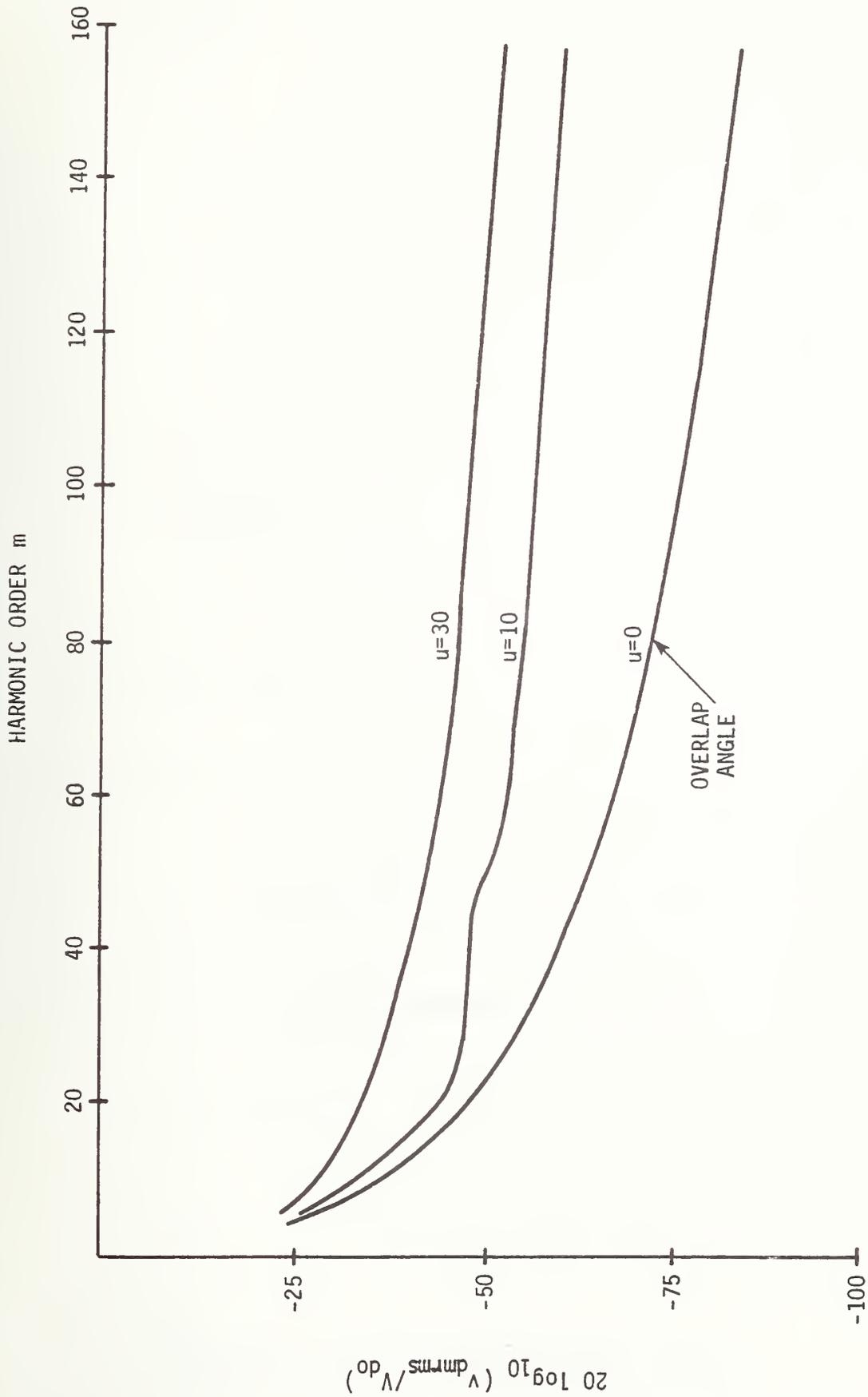
FIGURE 2-6. Variation of Harmonic Components with Overlap Angle

11
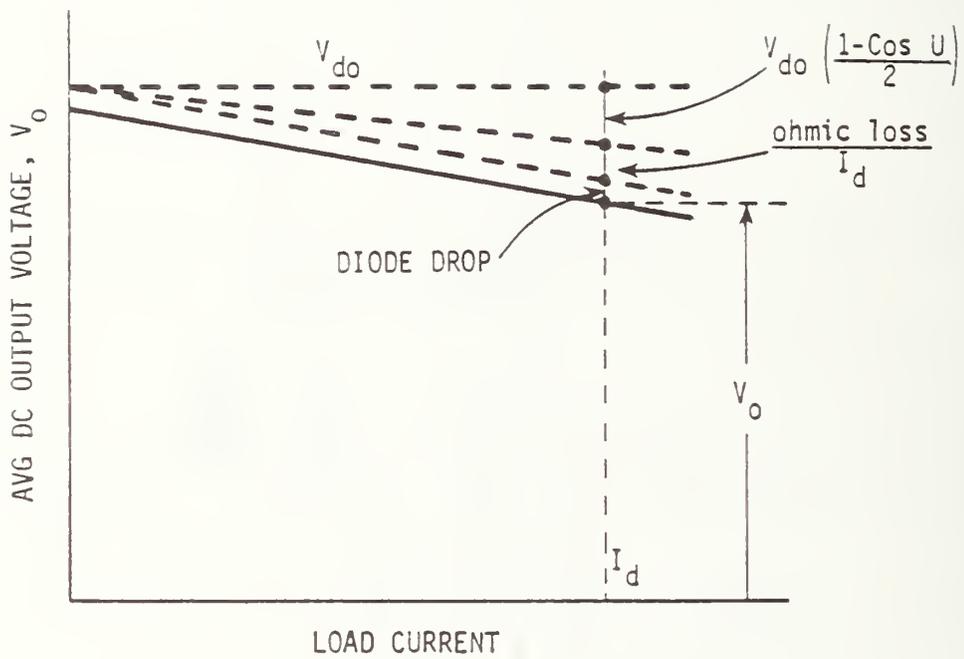
FIGURE 2-7. Voltage Regulation

12

contained harmonic components only of the order 6, 12, 18 . . . .6n of the source frequency. The three phase voltages are, however, never perfectly balanced. With unbalanced voltages, the dc output voltage contains harmonic components of the order 2,4,6,8, . . 2 n of the source frequency, because the overlap angles and the resulting diode conduction patterns are unsymmetrical, as shown in Figure 2-8; furthermore, if the six diode elements D1 - D6 of the rectifier are not identical, i.e., if the voltage drops across these elements for a given current are unequal, the output voltage then contains all the harmonic components. The bridge rectifier being a six pulse circuit, harmonic components of the order 6, 12, 18, ..6n are, of course, quite predominant.

Such an analysis of the operation of the rectifier with unbalanced input voltage appears in an Appendix to this report.

2.5 WAVEFORM OF AC NETWORK CURRENT

The line current waveforms of the rectifier appear in Figure 2-3. If the commutation process is considered, the current waveform can be represented as in Figure 2-9a, approximated by a trapezoidal waveform of Figure 2-9b. Mathematically the periodic function definition is:

$$f\{\theta\} = \frac{I_d}{u} (\theta + \frac{\pi}{3} + \frac{u}{2}) \quad \cdots \quad -\frac{\pi}{3} - \frac{u}{2} \leqslant \theta \leqslant -\frac{\pi}{3} + \frac{u}{2}$$

$$= I_d \quad \cdots \quad \frac{\pi}{3} + \frac{u}{2} \leqslant \theta \leqslant \frac{\pi}{3} - \frac{u}{2}$$

$$= \frac{I_d}{u} (\frac{\pi}{3} + \frac{u}{2} - \theta) \quad \cdots \quad \frac{\pi}{3} - \frac{u}{2} \leqslant \theta \leqslant \frac{\pi}{3} + \frac{u}{2}$$

13
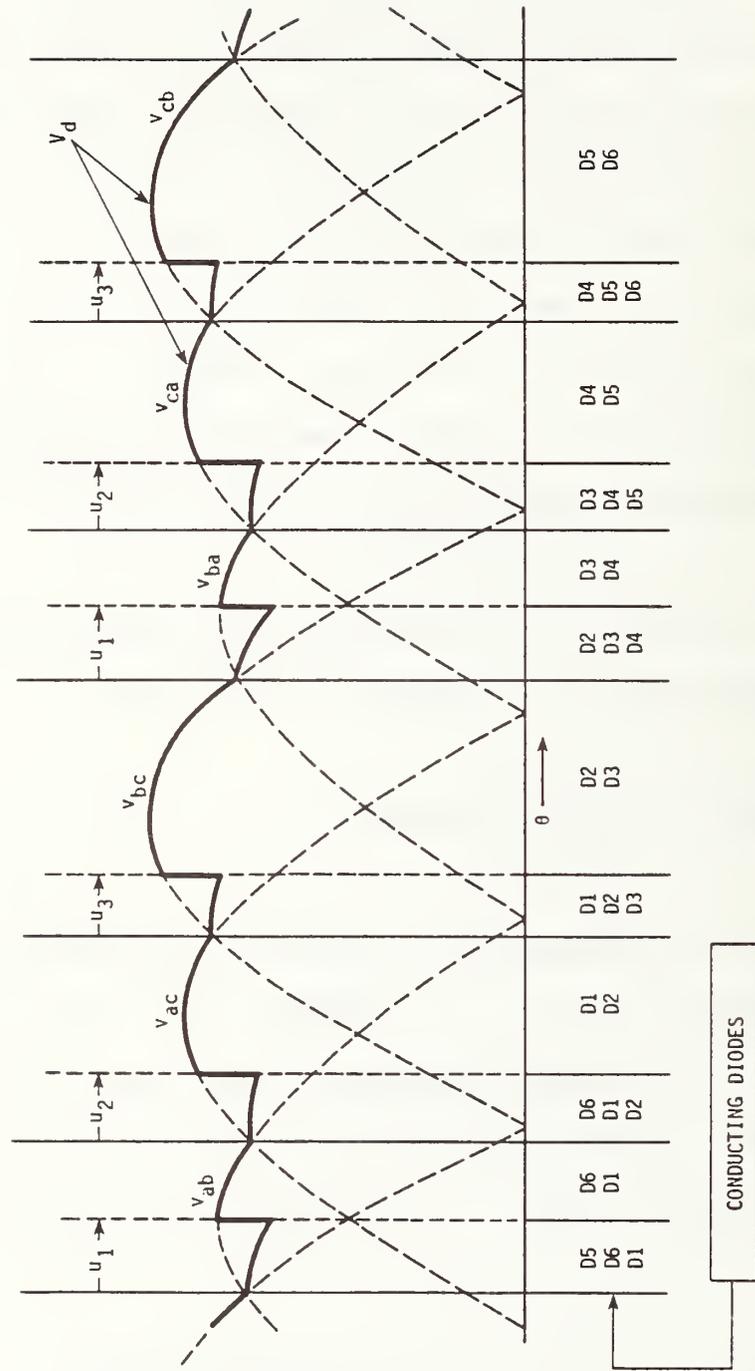
FIGURE 2-8. Operation with Unbalanced Voltage Input

14
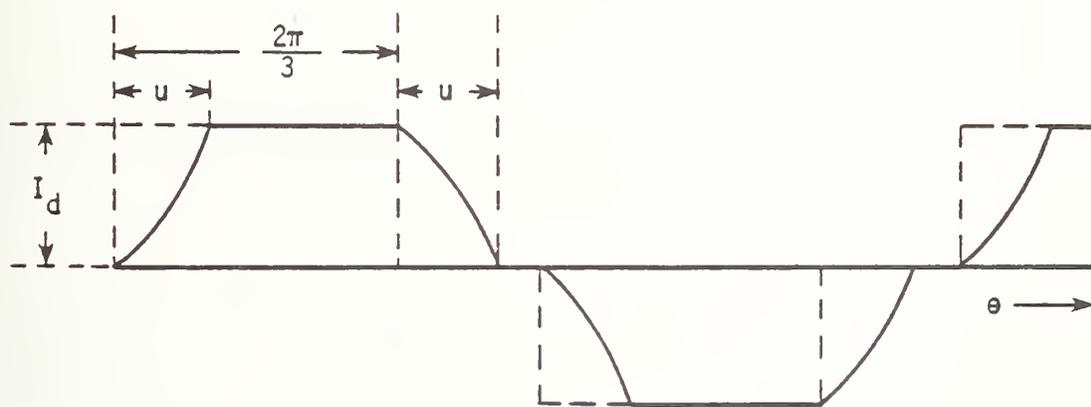
(a) ACTUAL
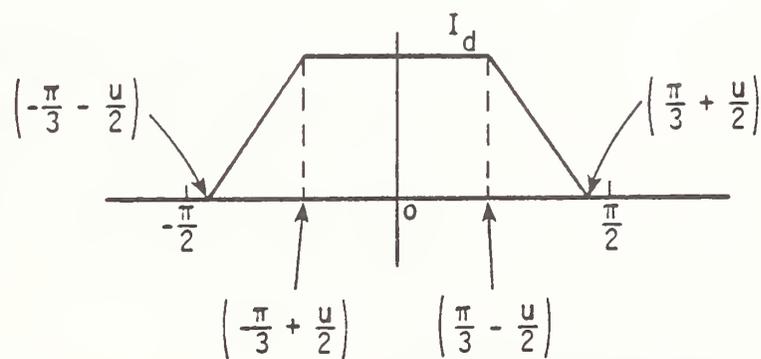
(b) APPROXIMATED

FIGURE 2-9. AC Waveform

15

The amplitude of the mth harmonic component of this current is given by

$$I_{mu} = \frac{4I_d}{\pi} \cdot \frac{Sin\left(\frac{m\pi}{3}\right)}{m} \cdot \frac{Sin\left(\frac{mu}{2}\right)}{\left(\frac{mu}{2}\right)}$$

If the commutation process is ignored, $u = o$ and then

$$I_{mo} = \frac{4I_d}{\pi} \cdot \frac{Sin\left(\frac{m\pi}{3}\right)}{m}$$

With these expressions some important conclusions can be drawn:

$$\frac{I_{mo}}{I_{10}} = \frac{1}{m}$$

with the harmonics of the order 5, 11, 17 . . .being out of phase with those of the order 1, 7, 13 . . . .etc.

Further $\qquad \dfrac{I_{mu}}{I_{mo}} = \dfrac{Sin\left(\frac{mu}{2}\right)}{\left(\frac{mu}{2}\right)} = f(m,u)$.

The function $f(m,u)$, quite well known, is plotted in Figure 2-10.

The current presented here is the one in the lines directly feeding the points a, b, c of the bridge circuit of Figure 2-1. If more than one rectifier are supplied by the ac network, lower orders of harmonics are effectively cancelled by properly phasing these rectifiers.

2.6 TWELVE PULSE RECTIFIER CIRCUITS

Higher pulse rectifier circuits are built by a series or parallel connection of two or more six pulse circuits having appropriate phase difference between the output voltages. A commonly used 12-pulse circuit appears in Figure 2-11 where two six pulse rectifiers are connected in

16
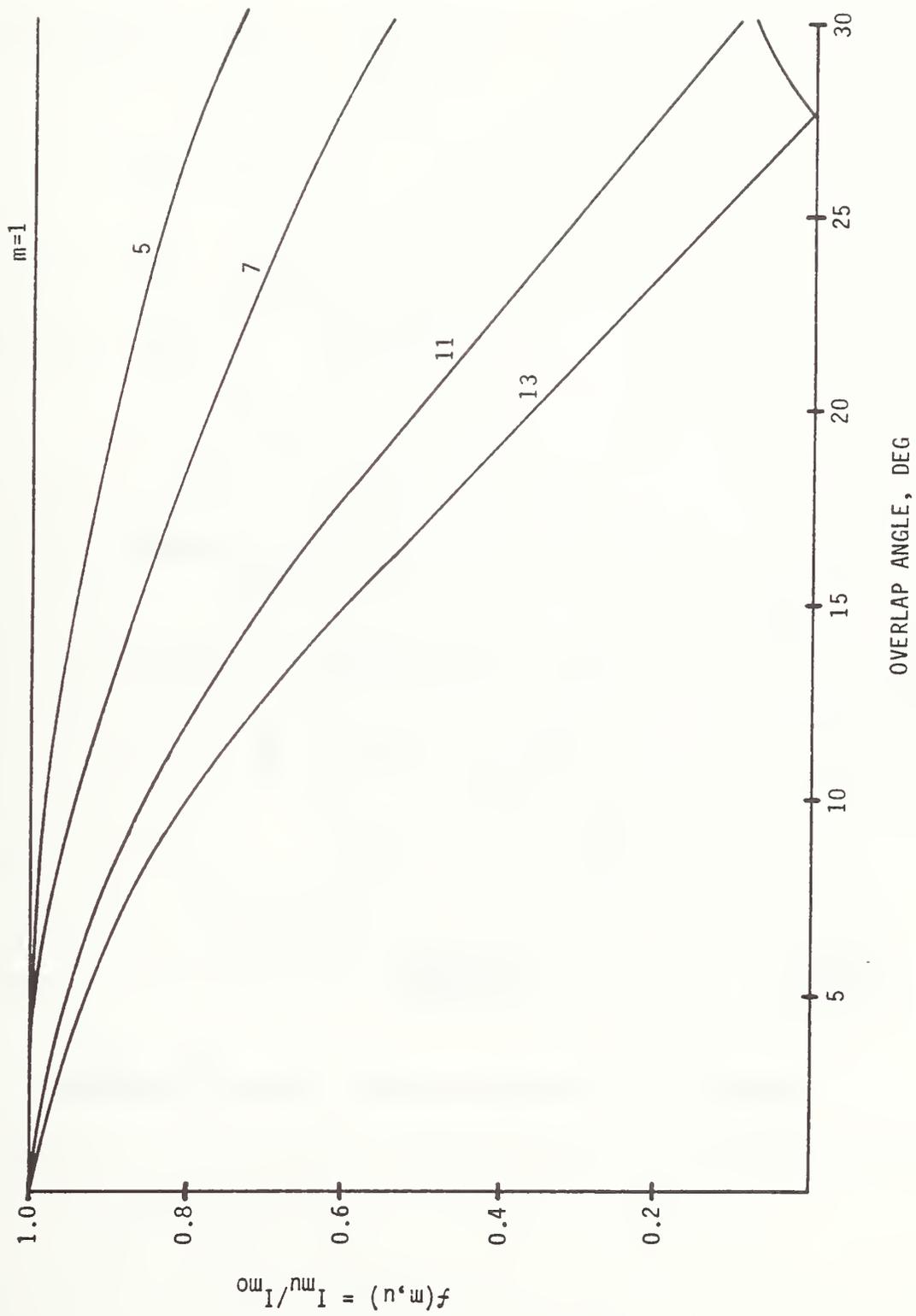
FIGURE 2-10. Effect of Commutation on AC Network Current

17
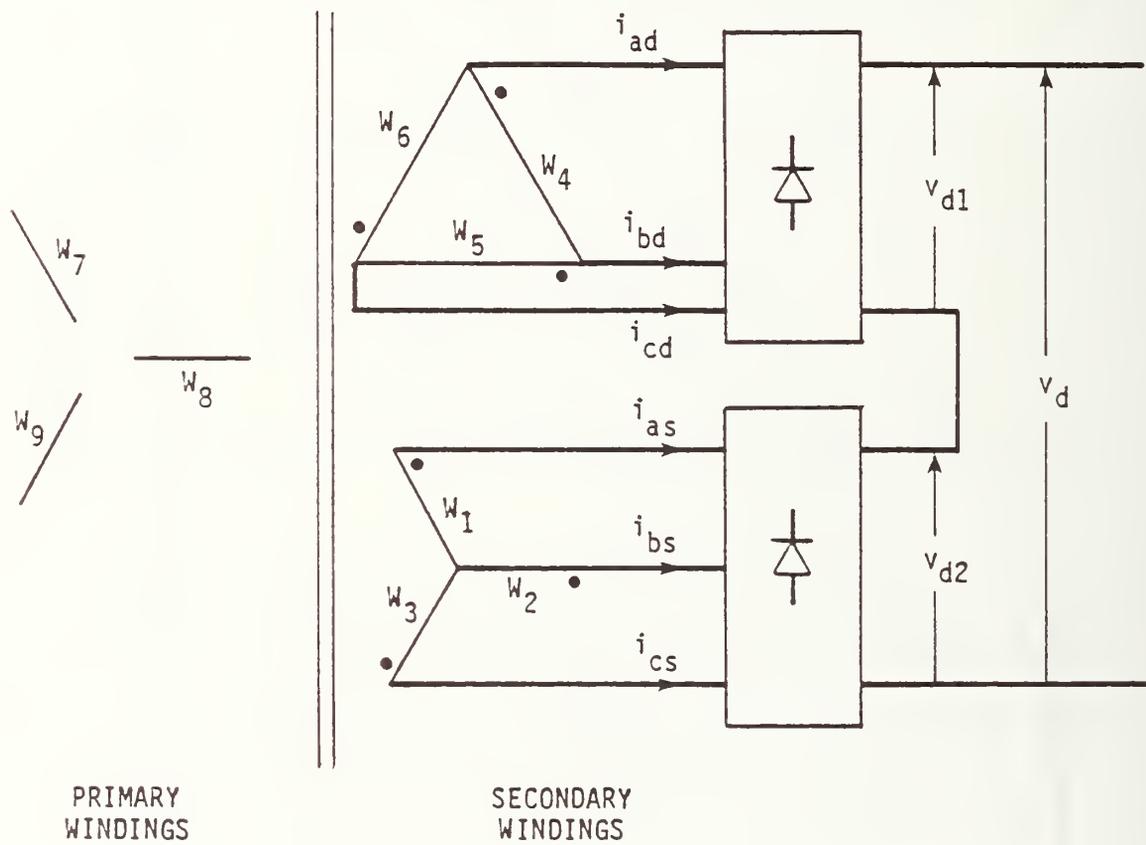
FIGURE 2-11.   A 12-Pulse Rectifier (Series Connection)

series.   A phase difference of 30° appears when two sets of secondary windings are used with one in delta and the other in a star connection.

The instantaneous output voltage of this circuit is:

$$v_d = v_{d_1} + v_{d_2} \; .$$

The resulting dc average voltage then appears as:

$$V_d = V_{d_1} + V_{d_2} \; .$$

Because V_{d_1} and V_{d_2} are shifted in phase by 30°, harmonic components with harmonic orders that are odd multiples of six are out of phase and are cancelled out.   The output voltage V_d, therefore, contains components with harmonic orders that are multiples of 12.   For a circuit supplied with 60Hz voltage source, therefore, the output contains harmonic components of frequencies 720, 1440, 2160 . .Hz.   The output voltage has a waveform shown in Figure 2-12.

If the line-to-line voltages of the two secondary sections are equal, the number of turns of the two sections must be related as

$$\frac{N_{w4}}{N_{w1}} = \frac{\sqrt{3}}{1}$$

One obtains the transformer winding current on the primary side by equating the ampere-turns as:

$$I_{w7}N_{w7} = I_{w1}N_{w1} + I_{w4}N_{w4}$$

$$I_{w7} = \frac{N_{w1}}{N_{w7}} \, (^1w1 + \sqrt{3} \; ^1w4).$$

19
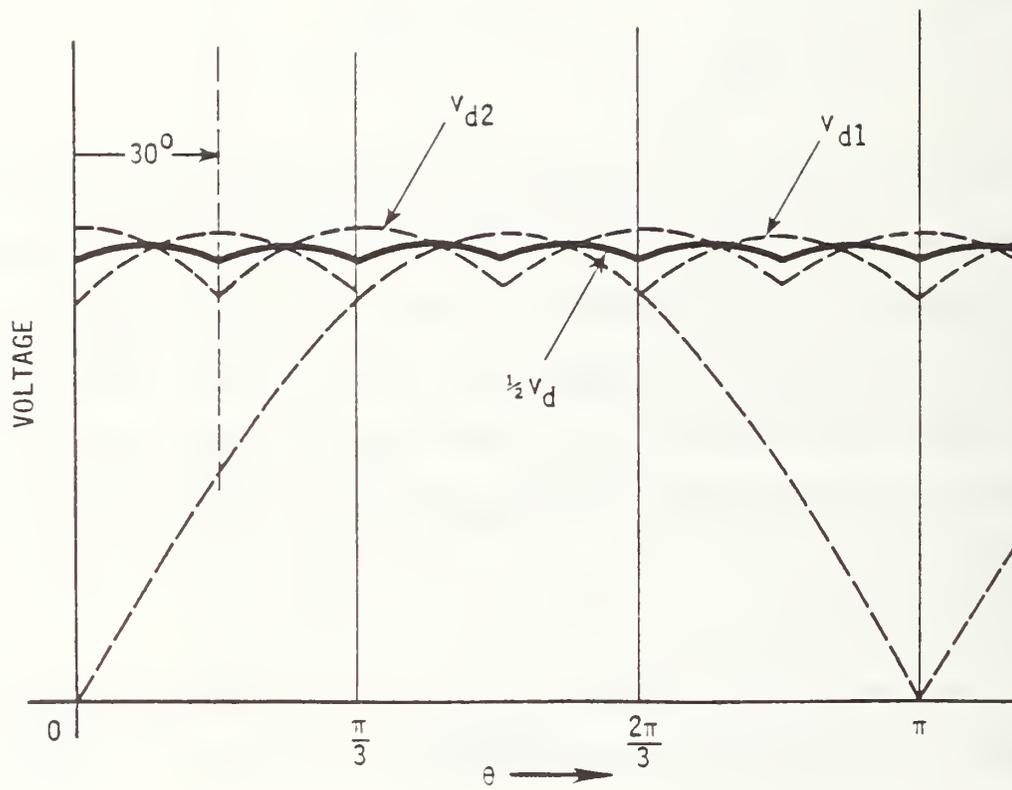
FIGURE 2-12. Output Voltage of 12-Pulse Circuit

The waveform of current through winding W_7 and other currents appear as shown in Figure 2-13. The rectifier circuit then appears as a 12-pulse circuit to the ac network, as well as to the dc side load.

The two six pulse rectifiers may also be connected in parallel to obtain a 12-pulse rectifier, as in Figure 2-14. Because the two output voltages are not identically equal, some reactances are necessary in the circuit to limit short circuit currents between the rectifiers. A center-tapped reactor, known as an interphase reactor, is normally used as shown. Any flux resulting from the dc component of the load current thus cancels out, making a light reactor design possible.

2.7 A CONTROLLED RECTIFIER/INVERTER CIRCUIT

When thyristors replace all the diodes in the bridge circuit of Figure 2-15, the output voltage can be varied continuously from $+V_{do}$ to $-V_{do}$, if commutation is instantaneous. With a finite reactance in the circuit, this range lessens, depending on the overlap angle.

One measures the firing angle α of the thyristors from the instant of diode conduction (Figure 2-15). α is also called the delay angle because the thyristor conduction is delayed by that angle. The commutation period, i.e., the overlap angle for a given delay angle, is given by

$$\text{Cos}\,(\alpha + u) = \text{Cos}\,\alpha - \frac{2X_c I_d}{V}$$

21
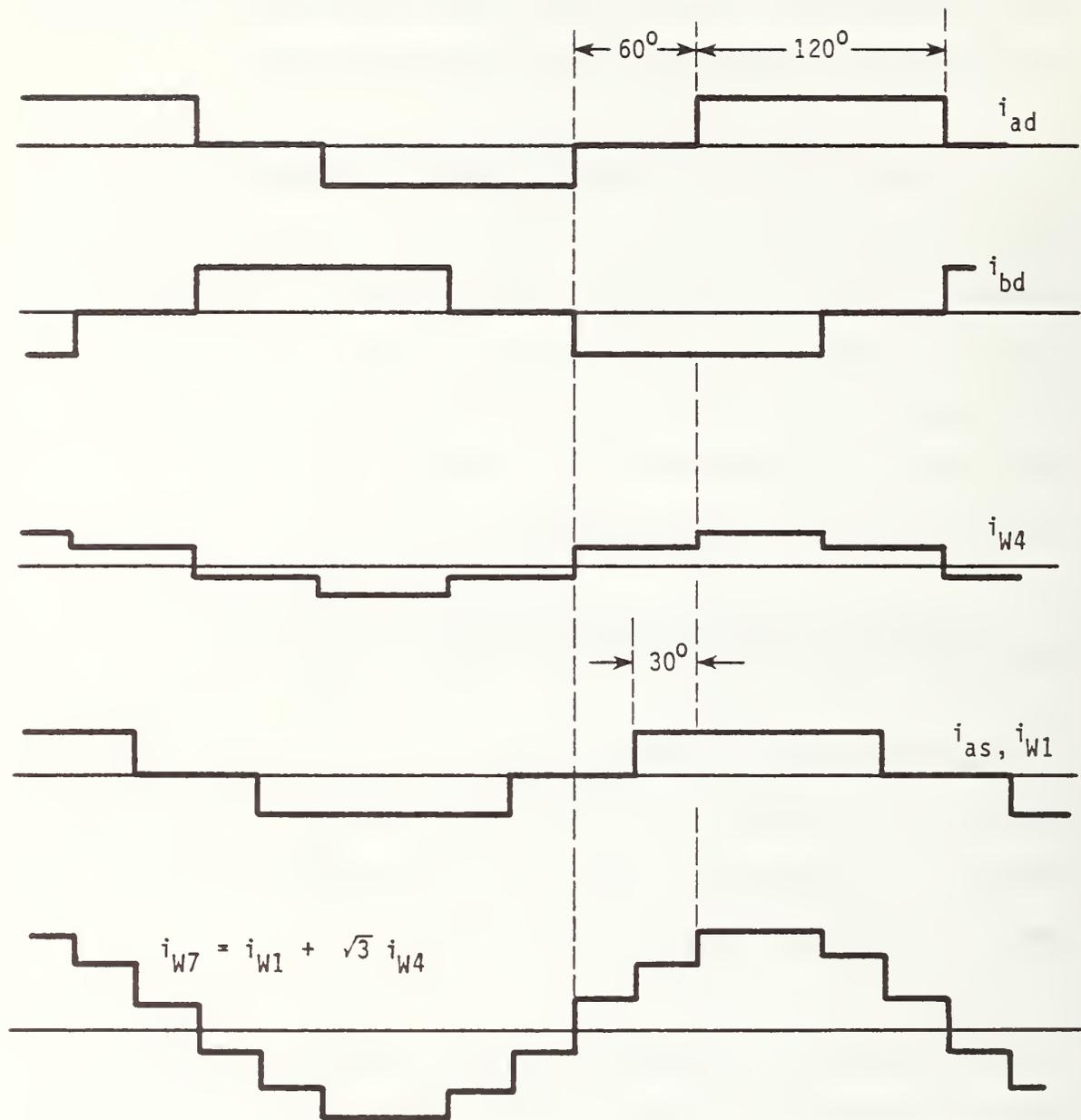
FIGURE 2-13. Currents in Different Windings

22
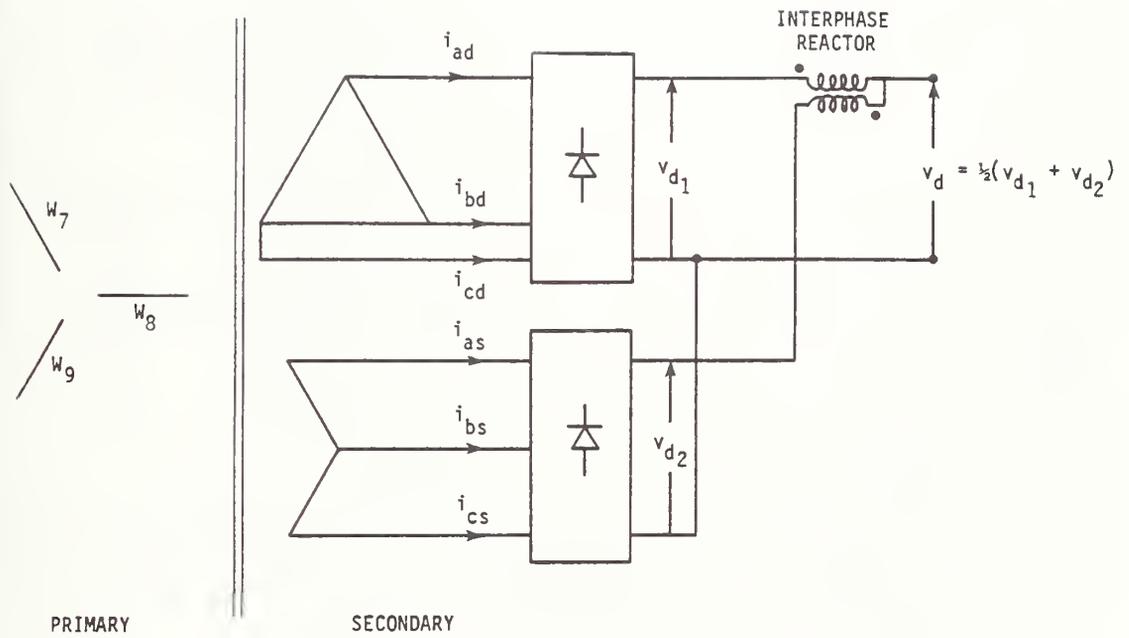
FIGURE 2-14. A 12-Pulse Rectifier (Parallel Connection)
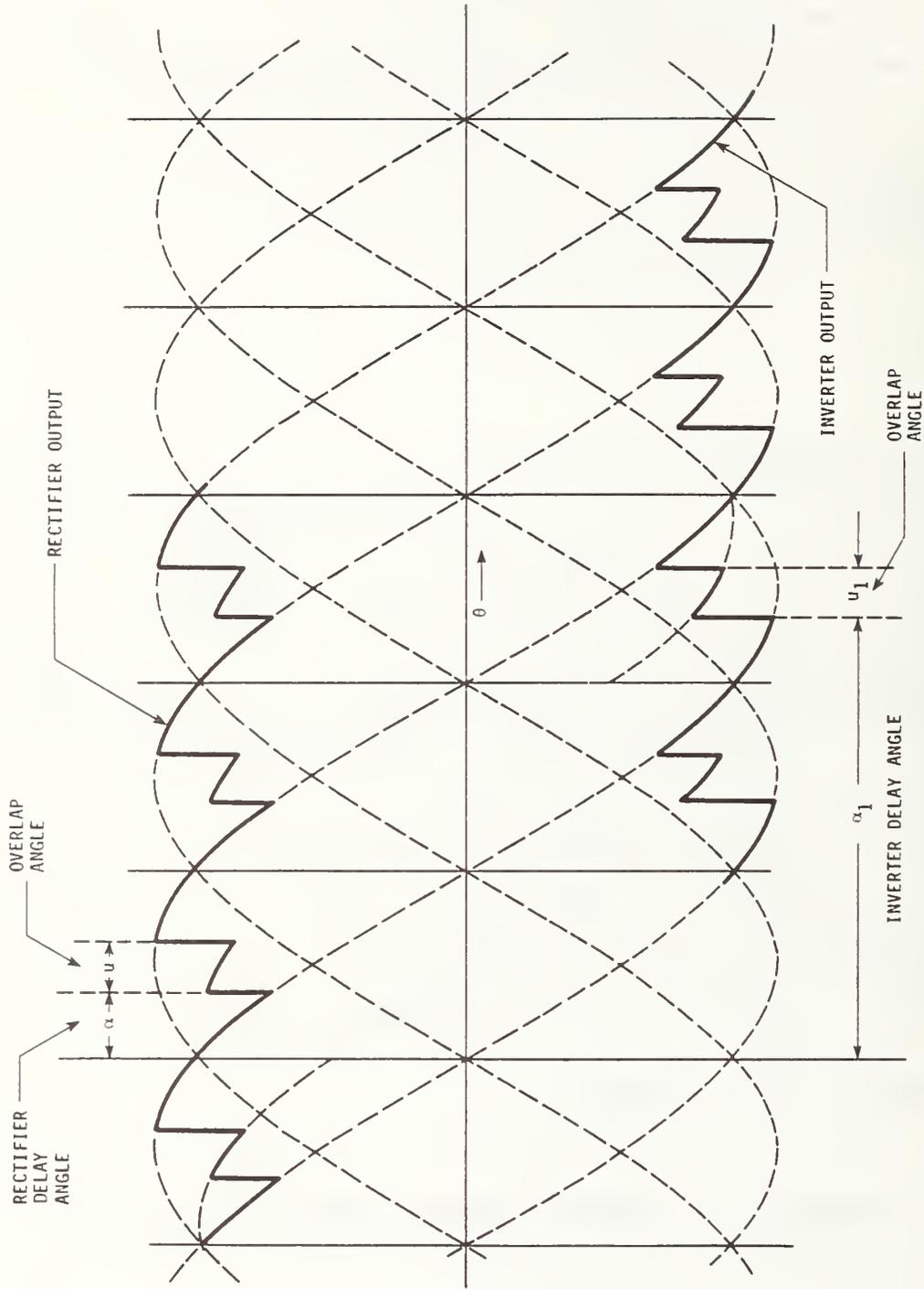
FIGURE 2-15. Operating Modes of a Controlled Rectifier

The voltage output now is:

$$V_d = V \sin \left(\alpha + u + \frac{\pi}{3} + \theta\right) \quad \ldots \quad 0 \leqslant \theta \leqslant \frac{\pi}{3} - u$$

$$= \frac{\sqrt{3}}{2} V \sin \left(\alpha + u + \frac{\pi}{6} + \theta\right) \ldots \quad \frac{\pi}{3} - u \leqslant \theta \leqslant \frac{\pi}{3}$$

The average value of this voltage is:

$$V_{d\alpha} = \frac{3V}{2\pi} [\cos \alpha + \cos (\alpha + u)]$$

and with u = 0

$$V_{d\alpha o} = \frac{3V}{\pi} \cos \alpha$$

As the delay angle increases from o to π, v_{do} goes from $+V_{do}$ to $-V_{do}$. When the output voltage of the circuit is negative, power flows from the dc side to the ac side. One then speaks of the circuit as inverting. Figure 2-15 clearly illustrates these operating modes.

The harmonic components of this waveform are:

$$V_{dm\ \alpha\ rms} = \frac{3V}{\pi(m^2-1)} \frac{1}{\sqrt{2}} \text{ MAG } [\cos \alpha + e^{jmu} \cos (\alpha + u)$$

$$-jm \{\sin \alpha + e^{jmu} \sin (\alpha + u)\}]$$

and are plotted in Figure 2-16. For $\alpha = u = o$, this expression reduces to an earlier one:

$$V_{dmrms} = \frac{3V}{\pi} \cdot \frac{\sqrt{2}}{m^2-1}$$

One must remember that 'm' is only a multiple of 6. Also, as the delay angle increases, the total harmonic content of the output voltage increases, although individual harmonic components may fluctuate over a significant range.
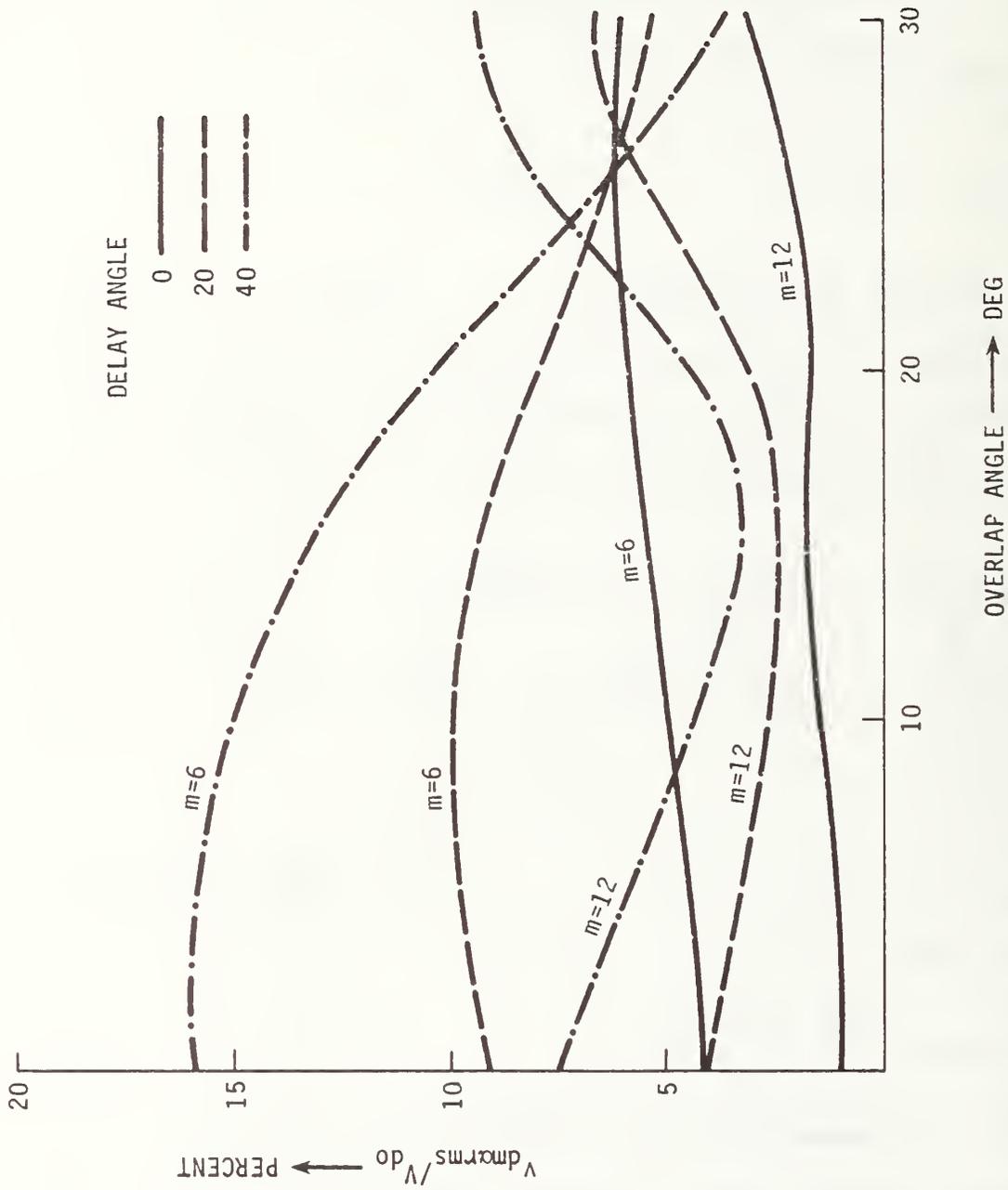
FIGURE 2-16. Harmonic Content of a Controlled Rectifier

Inverter circuits with higher pulse numbers are obtainable by series or parallel connection of one or more six pulse circuits, as previously explained.

2.8 RECTIFIER SUBSTATIONS FOR TRANSIT APPLICATION

A typical transit substation has two or more 6- or 12-pulse diode rectifiers with a combined power rating of 2-10 MW. In the United States two types of connections are widely used; one uses two separate 3 phase transformers with 30° phase shift supplying two bridge rectifiers connected in series or parallel, and the other uses a three winding transformer supplying two bridge rectifiers in series or parallel as shown in Figures 2-11 and 2-14. Both these connections result in a 12 pulse rectifier circuit.

The Japanese, however, widely use 6 pulse circuits and are also increasingly introducing inverter substations to ensure receptivity of the third rail/catenary for regenerated power during vehicle braking. Such inverter equipment is, however, not found in revenue service outside Japan, although some experimental units were built in Europe earlier.

3. SUBSTATION HARMONICS AND TRACK CIRCUITS [1,5,6,7]

Two basic ways exist in which harmonic currents resulting from operation of rectifier substations may cause potential interference with audio frequency track circuits used for train detection, cab signalling, and vehicle speed control. These are:

(a) conducted noise because of unbalance in propulsion return current in running rails, and

(b) voltages induced in the track circuit by current carrying third rail,

One must, therefore, obtain components of propulsion current of frequencies corresponding to substation harmonics.

3.1 SUBSTATION HARMONICS IN PROPULSION CURRENT

Figure 3-1 presents a circuit that carries the propulsion current. The equivalent circuit of the propulsion circuit also appears in the figure. The voltage e_{ms} is the rms value of the mth harmonic component of the rectifier output at the substation. The impedances, Z_s, Z_r etc., are the impedances of various components at the frequency under consideration.

The harmonic components e_{ms} of six and twelve pulse rectifiers have been presented earlier. Note that the actual direct current drawn by the train affects the value of e_{ms} only indirectly, via the commutation overlap angle.

(a) CIRCUIT COMPONENTS

(b) EQUIVALENT CIRCUIT

(c) CIRCUIT CONSTANTS
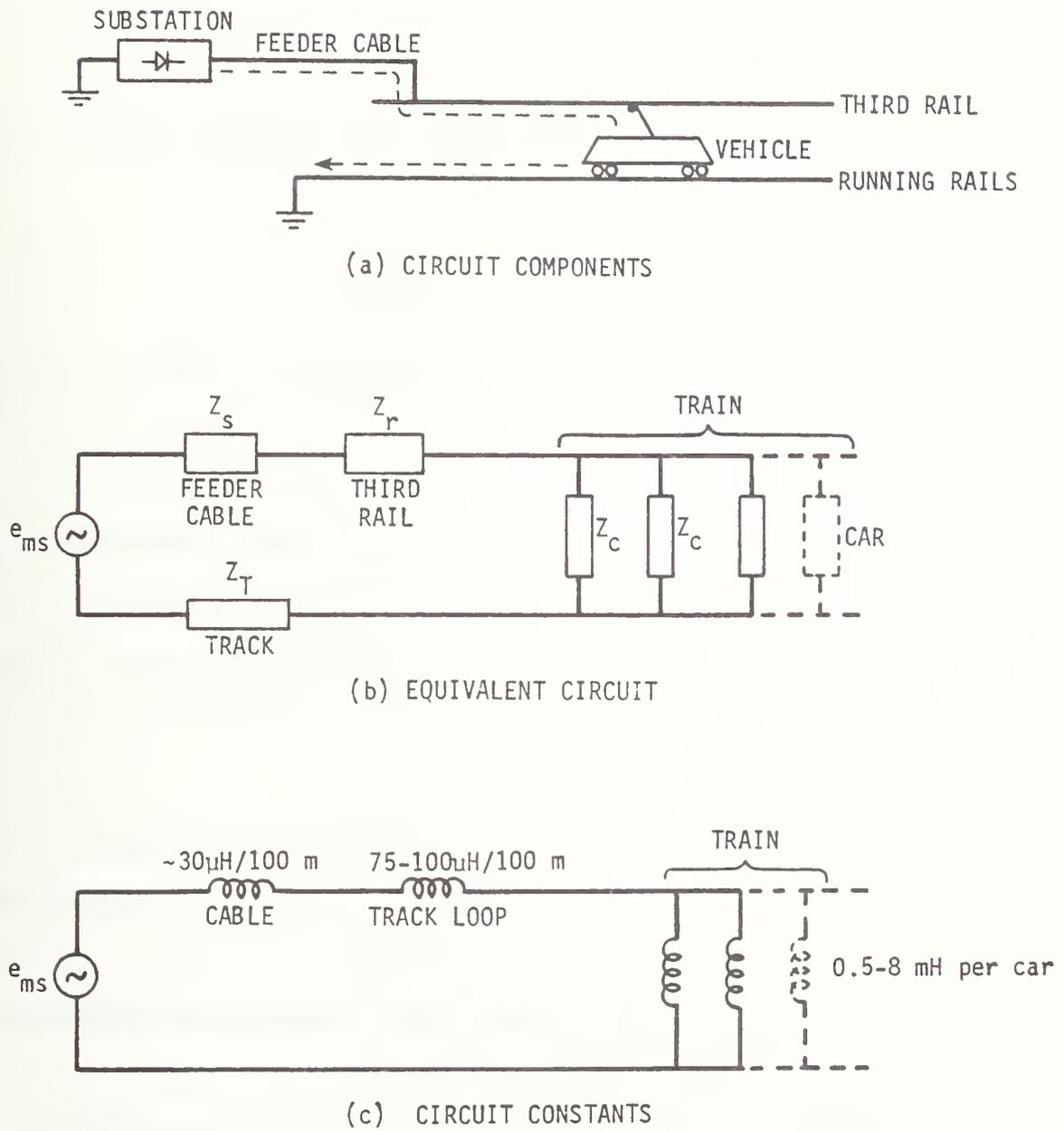
FIGURE 3-1. Substation Harmonics in Propulsion Current

The actual values of the impedances Z_s, Z_r etc., are very 'site specific'. However, the order of these impedances may be obtained as follows:

(a) <u>Feeder cable impedance Z_s</u> - This cable usually is a 750-2000 MCM cable with the impedances of the order of:

$R_{dc} \simeq 4 \cdot 2$ mΩ/100m and L $\simeq$ 30 μH/100m

The effective ac resistance at any frequency increases because of skin effect. For example, it may go up about 30 percent for 60 Hz, and for audio frequency range it may increase by a factor as great as 5-7. The effective ac inductance, however, reduces at higher frequencies, depending on the site topology. For audio frequency range of interest (2-10 kHz), therefore, one may consider the cable purely inductive.

(b) <u>Third rail and running rail impedances</u> - The dc resistance of these rails is of the order of 1-2 mΩ/100m, although the effective ac resistance is possibly of the order of 15-30 mΩ/100m in the audio frequency range (2-10 kHz). The inductance of these rails is in the range of 90-150 μH/100m for low frequencies and drops by about 20 percent in the audio frequency range. These rails are, however, electromagnetically linked, and customarily one considers an equivalent inductance of a loop formed by the third rail and the two running rails, instead of the individual self inductances. This loop inductance could be 75-100 μH/100m, with the lower range applicable to high

30

frequencies. In the audio frequency range of interest, the inductive reactance of these rails is 1-5 Ω/100m, much larger than the ohmic impedance.

(c) Car impedance - In chopper controlled or inverter controlled cars, an L-C line filter isolates the third rail from the propulsion equipment. In the audio frequency range, therefore, a car appears as a purely inductive impedance, in the range 0.5-8 mH per car, depending on the filter design.

The equivalent circuit of Figure 3-1b now appears as in Figure 3-1c. Considering the voltage unbalance on the ac side of the substation, the rms harmonic component e_{ms} of the rectifier output at rated load could be as high as 3.0 - 0.5 percent of the dc output for audio frequency range of 1 kHz-6 kHz (see Appendix).

One can thus estimate with fair accuracy the substation harmonic components of the third rail current.

3.2 CONDUCTED NOISE

Consider a track circuit as shown in Figure 3-2. The rails carry the propulsion return current as shown. The voltage drops across the running rails caused by the propulsion current appear as voltage sources for the track circuit. The drops across the running rails, in addition, oppose each other. The track circuit sees only the differential voltage as a noise source. The noise current i_{ns} in the receiver is then given by:

31
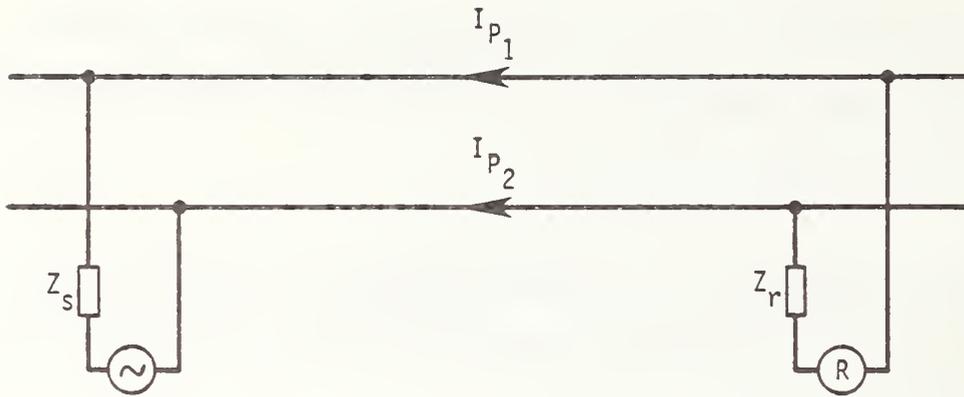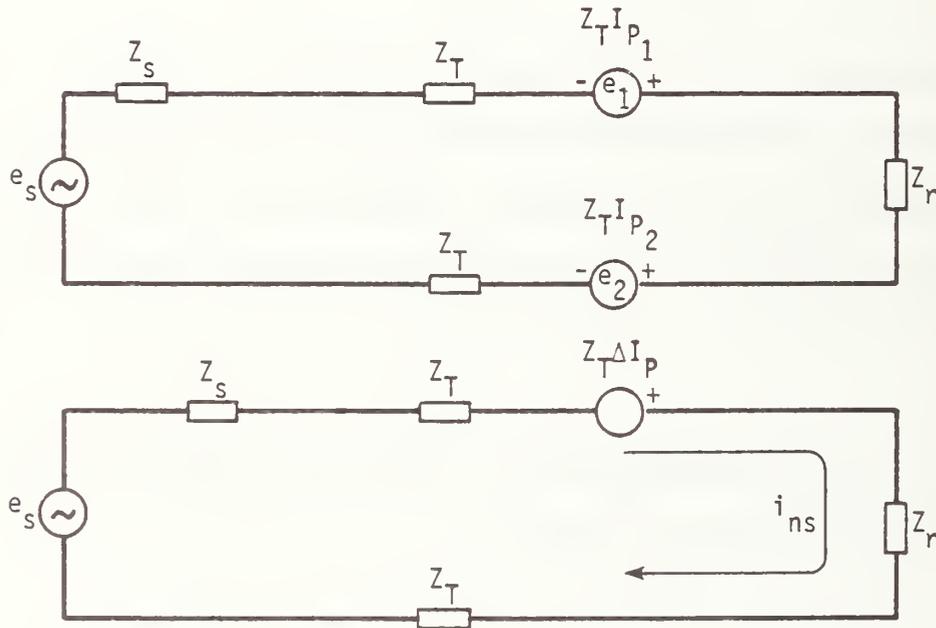
A. TRACK CIRCUIT

B. EQUIVALENT CIRCUITS

FIGURE 3-2.   Conducted Noise in a Track Circuit

$$i_{ms} = \frac{Z_T}{Z_s + 2 Z_T + Z_r} \cdot \Delta I_p$$

When Z_s, Z_T, Z_r are the impedances of the source, track per side and the receiver, respectively, and ΔI_p is the differential propulsion current. This equation is valid for any and each of the frequency components of ΔI_p.

For a double rail circuit one must also consider the effect of the track-train dynamics and the presence of flat wheels on a train. Any loss of wheel contact with a rail results in instantaneous transfer of propulsion current to the other rail still in contact with the other wheel on that axle. Similar transfer of current, in part or in full, possibly results when a wheel flat goes over a rail. The division of propulsion return current between the rails may, therefore, vary in time. The current unbalance ΔI_p and the conducted noise i_{sn} may, therefore, contain a series of bidirectional pulses of randomly varying amplitude, width, and frequency.

3.3 NOISE INDUCED FROM THE THIRD RAIL[1,6]

Consider the coupling between the third rail and a track circuit with reference to the geometry of Figure 3-3. The voltage e_{rms} induced in the track circuit is given by:

$$e_{rms} = \mu_0 \, f \, L \, I_{rms} \, \log_e \left[\frac{h^2 + (d+G)^2}{h^2 + d^2} \right]^{\frac{1}{2}}$$

A, B - RAILS
C - THIRD RAIL
G - RAIL GAGE
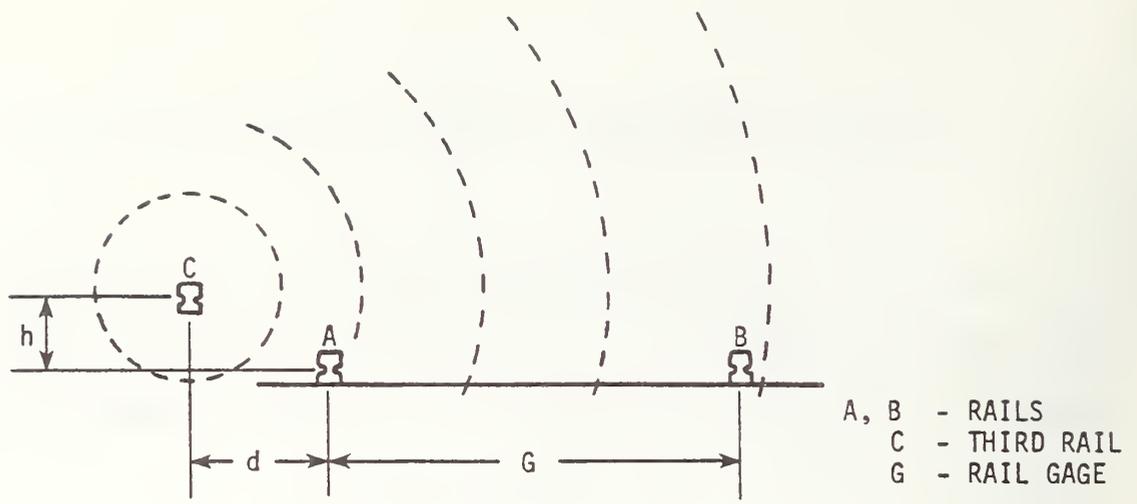
A. RAIL GEOMETRY
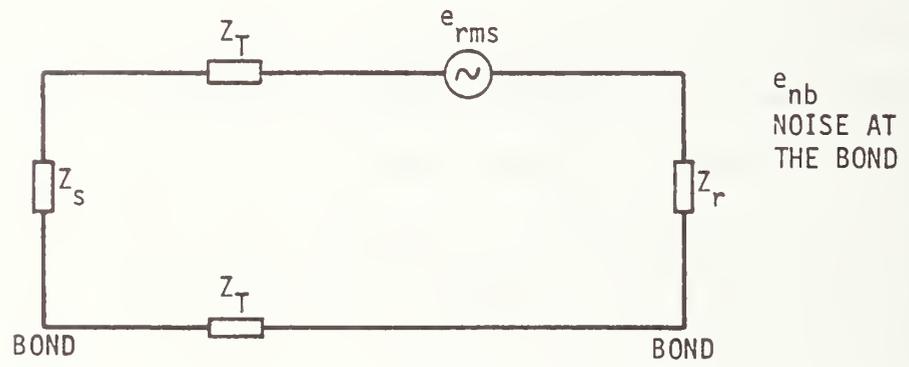
B. EQUIVALENT CIRCUIT

FIGURE 3-3. Noise Induction by the Third Rail

where I_{rms} is the current in the third rail with a frequency f and L is the length of the track circuit.

For long track circuits, the track impedance is quite large compared to the bond impedance; therefore, if L_u is the track circuit inductance per unit length, the noise current i_{ns} in the loop is:

$$\frac{i_{ns}}{I_{rms}} = \frac{e_{rms}}{2\pi f L_u L I_{rms}} = \frac{\mu_o}{2\pi L_u} \log_e [\frac{h^2 + (d \quad G)^2}{h^2 + d^2}]^{\frac{1}{2}}$$

This ratio is independent of frequency and track circuit length. For standard gage with G = 1.435 m and L_u = 1.3 μH/m, the ratio i_{ns}/I_{rms} is about 22 percent for d = h = 0.3m and about 14 percent for d = h = 0.6m.

Because each bond is a part of more than one track circuit, the noise current in the bond is not directly given by i_{ns}. Figure 3-4 shows different track circuit configurations, and for each configuration the current in the bond is different. One can, however, estimate rather accurately the current in the bond, as shown previously. Any possibility of unwanted pick up or drop of a track relay depends on the characteristics of the filter in the relay circuit, i.e., on the in-band component of the current in the bond.
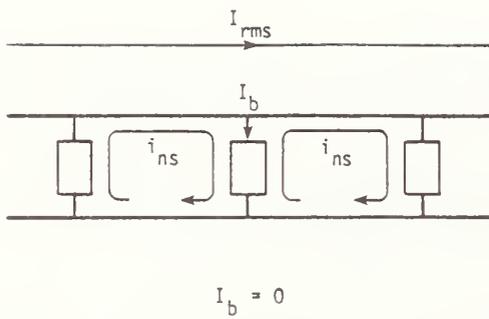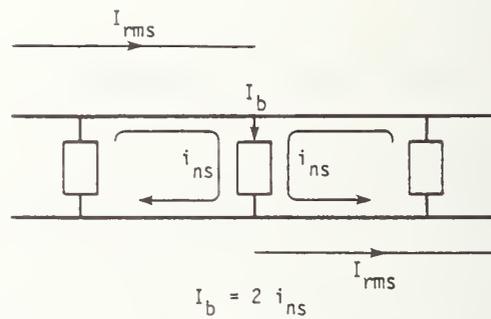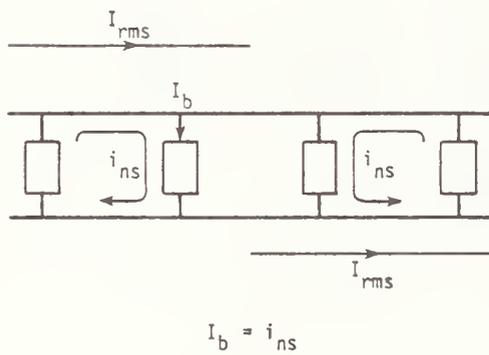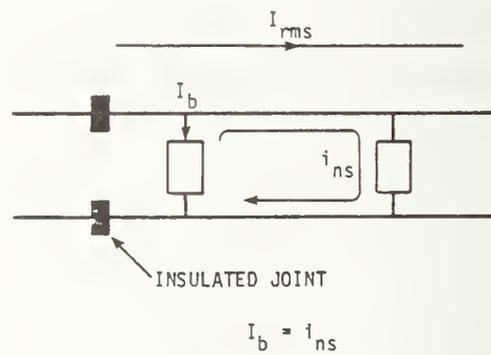
FIGURE 3-4. Track Circuit Configurations

3.4 ASSESSMENT OF POTENTIAL FOR INTERFERENCE

Electromagnetic noise at substation harmonic frequencies present in track circuits is caused by the basic rectifier operation and is independent of the type of onboard propulsion control. For example, such noise will be present in track circuits irrespective of whether the vehicles use cam-controlled or chopper-controlled dc drive, or inverter controlled ac drive. Each of this drive will, of course, cause additional EM noise (with commutator frequency, chopper harmonic frequencies, inverter harmonic frequencies, etc.), in track circuits according to its operating characteristics. But the potential interference problems caused by substation rectifier equipment can be investigated separately and independently of other noise sources.

The substation harmonic frequencies are well defined - all are multiples of the power source frequency (60 Hz in the U.S., 50 Hz and/or 60 Hz in Europe and Japan), although some are more predominant than the others depending on the rectifier circuit configuration. Also, the amplitudes of third rail harmonic currents are highest when a train is near a feeding point on the third rail. When the length of running rail in propulsion circuit is short, furthermore, the propulsion return current is more or less shared equally between the two rails, unless an abnormally severe imbalance between the two occurs because of loose connections or other factors. Protecting against substation harmonics in general is easy, except in site-specific problem areas, such as the third rail switching sides at bonds, etc., where a high percentage of third rail harmonic currents is induced in the track circuit. These must then be investigated on an individual basis.

4. CONCLUSIONS

When a basic six pulse rectifier circuit is supplied with a balanced three phase voltage source, the rectified output voltage contains harmonic components with frequencies 6f, 12f, 18f. . .etc. Two such six pulse circuits in series or parallel with a phase difference produce an effective pulse number of 12. The voltage then contains frequencies of only 12f, 24f, 36f,..,. If, however, the input voltages are not balanced and the bridge rectifier circuit is inherently unsymmetric, the output voltage has all harmonics - f, 2f, 3f,..., although components with frequencies 6f, 12f, 18f,..., are predominant.

Currents of substation harmonic frequencies may flow through impedance bonds of any track circuit either via a common ohmic path (conducted noise due to propulsion unbalance in running rails) or because of induction from the third rail. Any possibility of interference with normal track circuit operation depends on the level of noise and characteristics of track circuit receivers. The level of noise at substation harmonic frequencies can, however, be estimated with fair accuracy, and the track circuit protected, except under some site-specific abnormal conditions.

APPENDIX A

RECTIFIER OPERATION WITH UNBALANCED VOLTAGE INPUT

Let the bridge rectifier be supplied with a set of unbalanced voltages as shown in Figure A-1. The voltage output of the circuit then is as presented in Figure A-2.

The angles α's in the phasor diagram of Figure A-1 appear as:

$$\alpha_1 = 60 + \Delta_2$$

$$\alpha_2 = 60 - \Delta_2 + \Delta_1$$

$$\alpha_3 = 60 - \Delta_1,$$

where

$$\Delta_1 = \frac{\pi}{3} - \cos^{-1}\left(\frac{V_{ab}^2 + V_{bc}^2 - V_{ca}^2}{2\,V_{ab}V_{bc}}\right)$$

$$\Delta_2 = \cos^{-1}\left(\frac{V_{ab}^2 + V_{ca}^2 - V_{bc}^2}{2\,V_{ab}V_{ca}}\right) - \frac{\pi}{3}$$

The voltage V_1^* and the angle β_1 are:

$$V_1^* = \frac{1}{2}\sqrt{V_{ab}^2 + V_{ac}^2 + 2\,V_{ab}V_{ac}\cos\alpha_1}$$

and

$$\beta_1 = \cos^{-1}\left(\frac{V_{ab} + V_{ac}\cos\alpha_1}{2\,V_1^*}\right)$$

$$V_1^* = \tfrac{1}{2}(V_{ab} + V_{ac}) \quad \text{etc.}$$
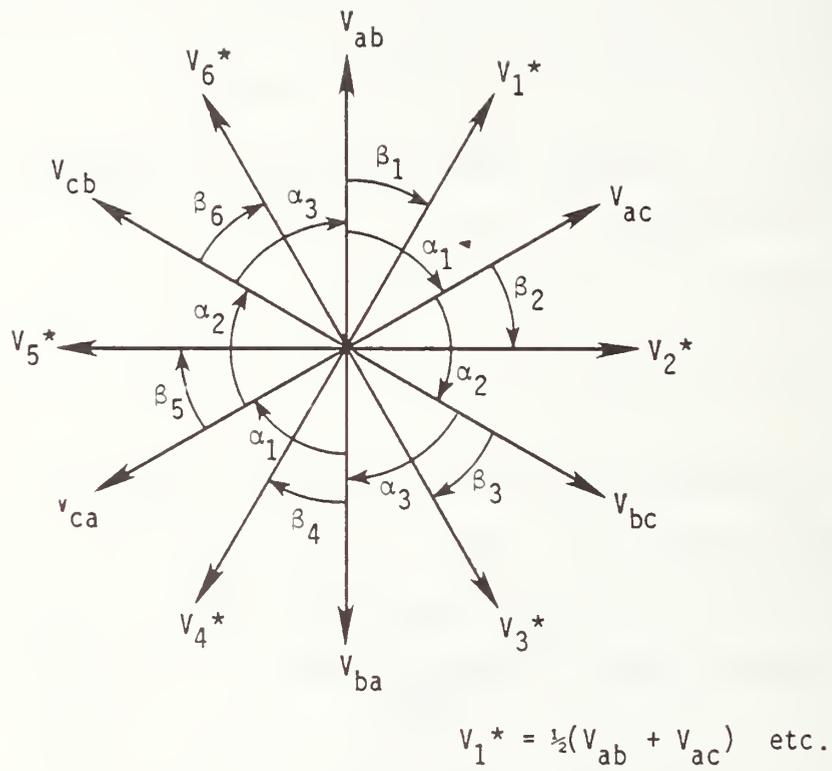
FIGURE A-1. Phasor Diagram
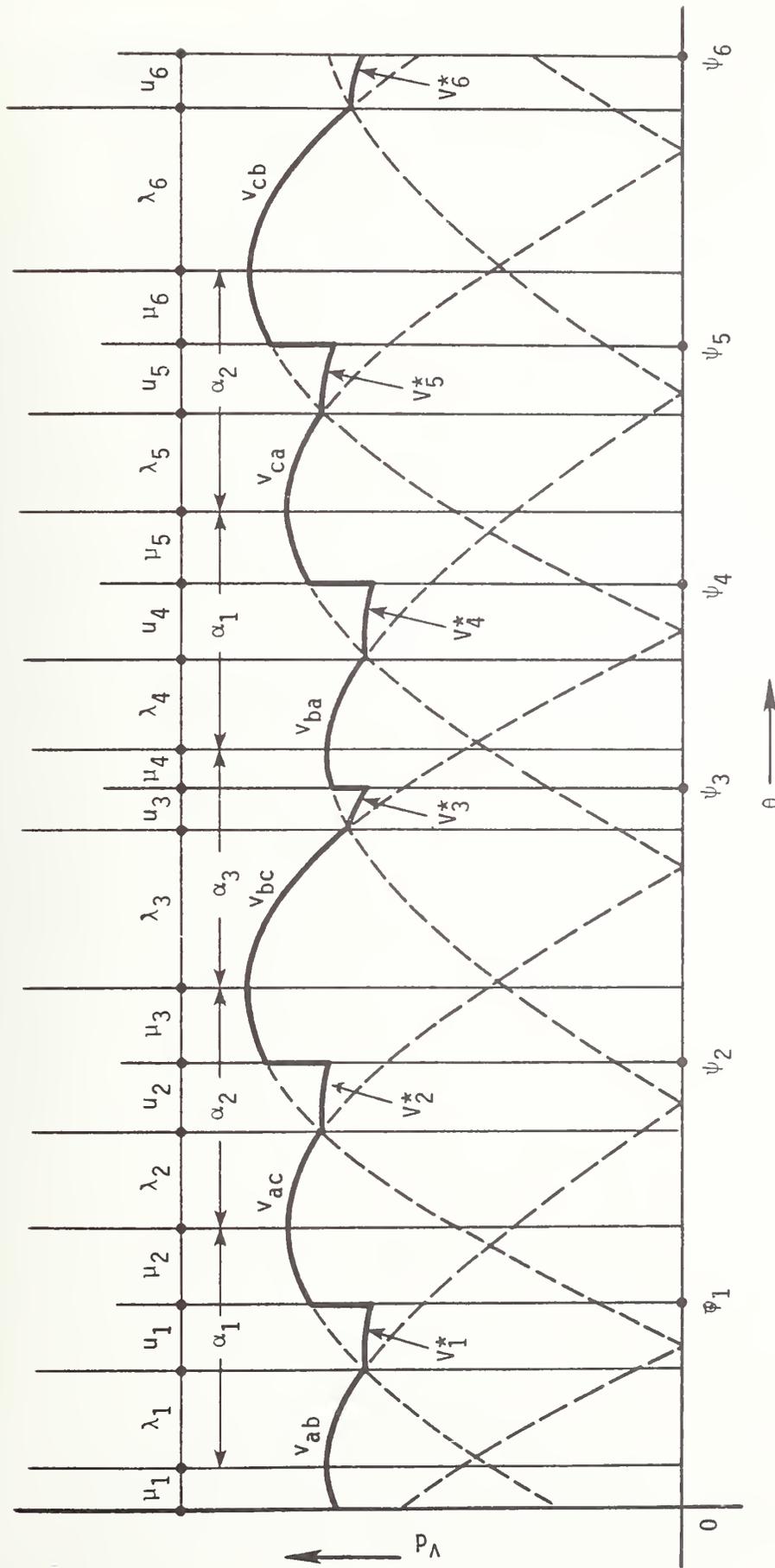
FIGURE A-2. Rectifier Operation with Unbalanced Voltage Input

41

Other voltages, such as V_2^*, V_3^*, and the angles β_2, β_3, are obtainable by noting the circular symmetry of the variables.

The overlap angles and other angles defining the conduction pattern can be obtained as:

$$\lambda_1 = Tan^{-1}(\frac{V_{ab} - V_{ac} \; Cos \; \alpha_1}{V_{ac} \; Sin \; \alpha_1})$$

$$u_1 = (\alpha_2 + \alpha_1 - \lambda_1) + Sin^{-1} [\; \frac{2X_c I_d}{V_{ac}} - Sin \; (\alpha_2 + \alpha_1 - \lambda_1) \;]$$

λ_2 -- λ_6 and U_2 -- u_6 may be obtained similarly.

One must define more angles before defining the rectifier output. These angles (see Figure A-2) are:

$$\mu_1 = \alpha_3 - \lambda_6 - u_6$$

$$\mu_2 = \alpha_1 - \lambda_1 - u_1$$

$$\mu_3 = \alpha_2 - \lambda_2 - u_2$$

$$\mu_4 = \alpha_3 - \lambda_3 - u_3$$

$$\mu_5 = \alpha_1 - \lambda_4 - u_4$$

$$\mu_6 = \alpha_2 - \lambda_5 - u_5$$

$$\Psi_1 = \mu_1 + \lambda_1 + u_1 \qquad = \Psi_1^*$$

$$\Psi_2 = \Psi_1 + \mu_2 + \lambda_2 + u_2 = \Psi_1 + \Psi_2^*$$

$$\Psi_3 = \Psi_2 + \mu_3 + \lambda_3 + u_3 = \Psi_2 + \Psi_3^*$$

$$\Psi_4 = \Psi_3 + \mu_4 + \lambda_4 + u_4 = \Psi_3 + \Psi_4^*$$

$$\Psi_5 = \Psi_4 + \mu_5 + \lambda_5 + u_5 = \Psi_4 + \Psi_5^*$$

$$\Psi_6 = \Psi_5 + \mu_6 + \lambda_6 + u_6 = \Psi_5 + \Psi_6^*$$

The output voltage $V_d(\Theta)$ now appears as:

$$
\begin{aligned}
V_d(\Theta) &= V_{ab} \cos(\Theta - \mu_1) & \cdots & & 0 \leqslant \Theta \leqslant \mu_1 + \lambda_1 \\
&= V_1^* \cos(\Theta - \mu_1 - \beta_1) & \cdots & & \mu_1 + \lambda_1 \leqslant \Theta \leqslant \Psi_1 \\
&= V_{ac} \cos(\Theta - \Psi_1 - \mu_2) & \cdots & & \Psi_1 \leqslant \Theta \leqslant \Psi_1 + \mu_2 + \lambda_2 \\
&= V_2^* \cos(\Theta - \Psi_1 - \mu_2 - \beta_2) & \cdots & & \Psi_1 + \mu_2 + \lambda_2 \leqslant \Theta \leqslant \Psi_2 \\
&= V_{bc} \cos(\Theta - \Psi_2 - \mu_3) & \cdots & & \Psi_2 \leqslant \Theta \leqslant \Psi_2 + \mu_3 + \lambda_3 \\
&= V_3^* \cos(\Theta - \Psi_2 - \mu_3 - \beta_3) & \cdots & & \Psi_2 + \mu_3 + \lambda_3 \leqslant \Theta \leqslant \Psi_3 \\
&= V_{ba} \cos(\Theta - \Psi_3 - \mu_4) & \cdots & & \Psi_3 \leqslant \Theta \leqslant \Psi_3 + \mu_4 + \lambda_4 \\
&= V_4^* \cos(\Theta - \Psi_3 - \mu_4 - \beta_4) & \cdots & & \Psi_3 + \mu_4 + \lambda_4 \leqslant \Theta \leqslant \Psi_4 \\
&\equiv V_{ca} \cos(\Theta - \Psi_4 - \mu_5) & \cdots & & \Psi_4 \leqslant \Theta \leqslant \Psi_4 + \mu_5 + \lambda_5 \\
&= V_5^* \cos(\Theta - \Psi_4 - \mu_5 - \beta_5) & \cdots & & \Psi_4 + \mu_5 + \lambda_5 \leqslant \Theta \leqslant \Psi_5 \\
&= V_{cb} \cos(\Theta - \Psi_5 - \mu_6) & \cdots & & \Psi_5 \leqslant \Theta \leqslant \Psi_5 + \mu_6 + \lambda_6 \\
&= V_6^* \cos(\Theta - \Psi_5 - \mu_6 - \beta_6) & \cdots & & \Psi_5 + \mu_6 + \lambda_6 \leqslant \Theta \leqslant \Psi_6
\end{aligned}
$$

This expression has been deliberately written in the most general terms to make the fundamental output frequency equal to the source frequency. Except for the different voltage drops (up to approximately 1 volt per diode) across the diode elements, however, the bridge circuit itself is quite symmetric, with the output voltage containing harmonics of the order 2, 4, ... 2n, etc.

The following equation represents the average value of the output as:

$$V_d = \frac{1}{2\pi} \int_o^{2\pi} v_d(\Theta) \, d\Theta$$

This integral computes as:

$$
\begin{aligned}
V_d = \frac{1}{2\pi} \Big[&\{V_{ab}(Sin\lambda_1 + Sin\mu_1) + V_1^* \{Sin(\Psi_1^* - \mu_1 - \beta_1) - Sin(\lambda_1 - \beta_1)\} \\
&+ V_{ac}(Sin\lambda_2 + Sin\mu_2) + V_2^* \{Sin(\Psi_2^* - \mu_2 - \beta_2) - Sin(\lambda_2 - \beta_2)\} \\
&+ V_{bc}(Sin\lambda_3 + Sin\mu_3) + V_3^* \quad Sin(\Psi_3^* - \mu_3 - \beta_3) - Sin(\lambda_3 - \beta_3)\} \\
&+ V_{ba}(Sin\lambda_4 + Sin\mu_4) + V_4^* \{Sin(\Psi_4^* - \mu_4 - \beta_4) - Sin(\lambda_4 - \beta_4)\} \\
&+ V_{ca}(Sin\lambda_5 + Sin\mu_5) + V_5^* \{Sin(\Psi_5^* - \mu_5 - \beta_5) - Sin(\lambda_5 - \beta_5)\} \\
&+ V_{cb}(Sin\lambda_6 + Sin\mu_6) + V_6^* \{Sin(\Psi_6^* - \mu_6 - \beta_6) - Sin(\lambda_6 - \beta_6)\} \Big]
\end{aligned}
$$

The amplitudes of other harmonic components are

$$V_{dm} = \underset{of}{Magnitude} \{ \frac{1}{\pi} \int_o^{2\pi} v_d(\Theta) \cdot e^{jm\Theta} \, d\Theta \}$$

This integral is very complex, but a typical integral of this type is evaluated in the example below. All the components of the above integral are obtainable similarly.

$$I = \int_{L}^{H} \cos(\Theta - A)\, e^{jm\Theta}\, d\Theta$$

$$= \frac{1}{m^2 - 1} \{-\sin(H-A)\, e^{jmH} + \sin(L-A)\, e^{jmL}$$

$$-jm\cos(H-A)\, e^{jmH} + jm\cos(L-A)\, e^{jmL}\,\}$$

$$\ldots \text{ for } m \neq 1$$

$$= \frac{H-L}{2}\, e^{jA} - \frac{j}{4}\, \{e^{j(2H-A)} - e^{j(2L-A)}\,\} \ldots \text{ for } m = 1$$

A computer program was prepared to compute the harmonic components of the rectifier output as defined above. Computations were made for voltage unbalance of up to 3 percent between the line voltages and an overlap corresponding to $X_c I_d / V_{phrms}$ of up to 15 percent. The results indicate that for audio frequency range of interest, i.e., harmonic orders between 18-100, the rms harmonic components can be as high as 0.5 - 3.0 percent, with the higher percentage corresponding to the lower frequencies.

REFERENCES

1.   Nene, V.D., "Electromagnetic Interference Characteristics of Advanced Propulsion Systems for Urban Rail Vehicles", Urban Mass Transportation Administration Report UMTA-VA-06-0075-81-1, 1981.

2.   Frasco, L., et al., "Electromagnetic Compatibility of Advanced Propulsion Systems", Proc. of the International Conference on Advanced Propulsion Systems, February 5-6, 1980. Urban Mass Transportation Administration Report No. DOT-UMTA-VA-06-0053-80-1, 1980. pp. 193-213.

3.   Holmstrom, F. Ross, "Chopper Induced Interference in Audio Frequency Track Circuits, "Urban Mass Transportation Administration Report No. UMTA-MA-06-0025-80-5, 1980.

4.   Holmstrom, F. Ross, "Comparisons of Inductive Chopper Interference from MARTA, BART, and NYCTA," Presented at TSC Rail Transit EMI meeting, San Francisco, California, June 1980.

5.   Amler, J., "The Effects of the DC-Chopper Technology in Public Rapid Transit Passenger Transport (PRTPT) - Summary," report by Verkehrs-Aktiengesellschaft, Nurnberg, Germany, 1978.

6.   Hoelscher, J., "Electromagnetic Coupling between the Third Rail and Track Circuits," - a private communication.

7.   Rudich, R., "Conducted Emissions" Garrett AiResearch Mfg. Co. Memo No. 81-17750, presented at Rail Transit EMI Technical Working Group meeting at Transportation Systems Center, Cambridge, Massachusetts, 24 January 1981.

APPENDIX B

REPORT OF NEW TECHNOLOGY

This report develops a method for estimating electromagnetic noise received by track circuits from rectifier substations. This method had not previously been published.

200 copies

HE 18.5 .A3

UMTA- 81-

Nene, Vilas

Harmonic ch

rectifier

Official Business
Penalty for Private Use $300

U.S.MAIL